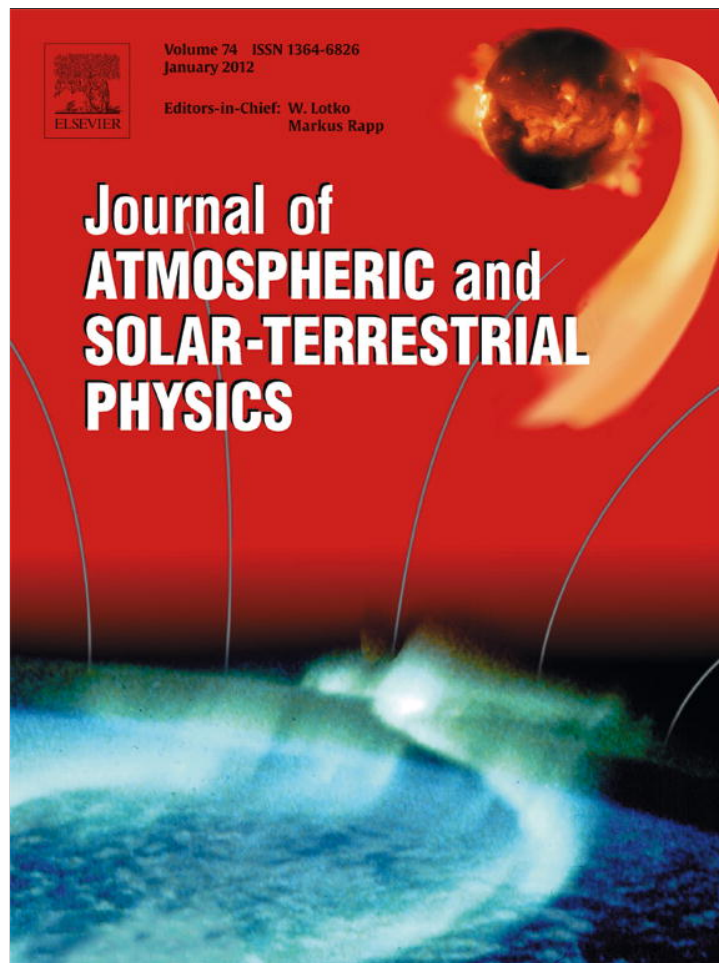


Provided for non-commercial research and education use.
Not for reproduction, distribution or commercial use.



(This is a sample cover image for this issue. The actual cover is not yet available at this time.)

This article appeared in a journal published by Elsevier. The attached copy is furnished to the author for internal non-commercial research and education use, including for instruction at the authors institution and sharing with colleagues.

Other uses, including reproduction and distribution, or selling or licensing copies, or posting to personal, institutional or third party websites are prohibited.

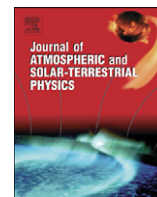
In most cases authors are permitted to post their version of the article (e.g. in Word or Tex form) to their personal website or institutional repository. Authors requiring further information regarding Elsevier's archiving and manuscript policies are encouraged to visit:

<http://www.elsevier.com/copyright>



Contents lists available at SciVerse ScienceDirect

Journal of Atmospheric and Solar-Terrestrial Physics

journal homepage: www.elsevier.com/locate/jastp

Analyses of the effects of several earthquakes on the sub-ionospheric VLF–LF signal propagation

S.S. De^{a,*}, Suman Paul^a, D.K. Haldar^a, D. De^b, A.K. Kundu^a, S. Chattopadhyay^a, S. Barui^a^a Centre of Advanced Study in Radio Physics and Electronics, University of Calcutta, 1, Girish Vidyaratna Lane, Kolkata 700 009, India^b Bengal Institute of Technology, Tech Town, Basanti Highway, Kolkata, India

ARTICLE INFO

Article history:

Received 23 December 2011

Received in revised form

2 March 2012

Accepted 9 March 2012

Available online 20 April 2012

Keywords:

Earthquake

Seismoelectromagnetism

Subionospheric propagation

Ionospheric perturbations

ABSTRACT

The precursory effects from several earthquakes upon the two subionospheric transmitted signals, one 19.8 kHz from North West Cape, Australia (lat: 21.82°S; long: 114.16°E) and the other 40 kHz from Fukushima, Japan (lat: 37.37°N; long: 140.85°E), are studied from the recorded data at Kolkata (lat: 22.56°N, long: 88.5°E). Some spiky transients are observed. Spike height and spike intensity are dependent on the depth of epicenter, distance of the epicenter from the propagation path and also from the observing station. The earthquakes occurring during the period of March 20, 2010–May 31, 2010 have been considered. Among 22 earthquakes, the analyses are made for only 13 earthquakes all having $M > 6$. Earthquake induced time-series observations of the spikes and their analyses are presented in this paper. Attempts are made to determine the possible visual study between M/D ratio and spike height. From this ratio, the probable sensitivity of the signals from different earthquakes may be studied.

© 2012 Elsevier Ltd. All rights reserved.

1. Introduction

An earthquake around its great-circle path can influence LF signals. The phase assimilation analysis of the effective magnitude of signals yields the information on ionospheric disturbances. The magnitude M is determined from the total energy of different earthquakes within the sensitive areas. When the transmitted signals during their propagation through the lower ionosphere get disturbed by the amplitude and phase anomaly, the effective magnitude would be greater ($M > 6$) and perturbation would take place 2–8 day prior to an earthquake. The dispersion in the medium would be very strong.

Electromagnetic phenomenon is observed at a place prior to any large earthquake ($M > 6$) along with the seismic effects within the lithosphere and ionosphere via atmosphere. The ionosphere gets perturbed with the seismic waves and there will be seismo-ionospheric coupling (Hayakawa and Molchanov, 2002; Hayakawa, 2004; Molchanov and Hayakawa, 2008). These waves are propagated in the form of precursory signals. Sub-ionospheric VLF/LF propagation has been extensively used to investigate seismo-ionospheric perturbation (Hayakawa, 2007; Hayakawa et al., 2010).

The evidence of ionospheric perturbation during Kobe earthquake was detected by using VLF transmitted signals (Hayakawa et al.,

1996). The irregular shifts in terminator time had been observed from several days prior to the earthquake date. The shifts during morning and evening period are interpreted in terms of lowering of the ionospheric height by several kilometers initiated by ionospheric perturbation caused by large earthquakes ($M > 6$).

In the event of large earthquakes, the ground layer atmosphere becomes ionized that produces ion acceleration, which, in turn, excites local plasma instabilities. The electron density of plasma in the upper ionosphere over the epicenter also increases extraordinarily. Therefore, an interrelation between the tectonic activity and the anomalous changes of the different geomorphical parameters of the Earth's lithosphere would develop. Ion and plasma concentration during the process of lithosphere–ionosphere coupling varies with the magnitude of the earthquake.

Several studies showed that the destructive earthquake on September 7, 1999 in Athens, Greece (lat: 38.2°N, long: 23.6°E) produced electromagnetic anomalies covering wide range of frequencies (Eftaxias et al., 2000; Karakelian et al., 2000; Eftaxias et al., 2001; Kapiris et al., 2002; Pham and Geller, 2002; Eftaxias et al., 2003). Spiky nature of the transient electromagnetic signals at 3 kHz frequency was detected which is similar to the VLF pre-seismic signals of Kozani–Grevena earthquake (Eftaxias et al., 2002). Similar records as regards VLF frequencies were reported for the 1995 Hyogo–Ken Nanbu earthquake (Izutsu and Oike, 2003; Izutsu, 2007). The VLF–VHF electromagnetic anomalies were also detected in case of large earthquake ($M=6.6$) of Kozani–Grevena in Greece (Eftaxias et al., 2000).

* Corresponding author. Tel.: +91 33 2350 5829; fax: +91 33 2351 5828.
E-mail address: de_syam_sundar@yahoo.co.in (S.S. De).

Some other important results on pre-seismic electromagnetic signals in the VLF/LF range are known (Ohta et al., 2001; Asada et al., 2001; Hattori, 2004).

The emission of electromagnetic noise is one of the important effects of earthquakes. This can be studied by examining whether the normal diurnal variation of VLF signal is hampered or by examining whether there are superpositions of VLF noise of large magnitudes. Accordingly, we have chosen two VLF signals along two different paths.

Although, researches studying the effects of earthquakes on VLF transmitted signals are plenty, no attempts are made to explore different aspects of 22 earthquakes which occurred within the span of 73 days. Among these, 13 are of $M > 6$ while the simultaneous shocks from other earthquakes are of lower M values ($M < 6$). These types of geophysical phenomena are uncommon which are presented in this paper for the first time. Some significant effects in the observations on VLF transmitted signals at frequencies 19.8 kHz and 40 kHz, recorded near Kolkata, for 22 large earthquakes of different magnitudes, location and depths are presented. A visual survey on the effects of these earthquakes on these sub-ionospheric VLF propagations has been reported in this paper. We have taken the wave path of two transmitted signals, one is of 19.8 kHz transmitted from Australia and the other of 40 kHz transmitted from Japan. Two such subionospheric transmitted signals are chosen because their propagational paths to the receiver crossed the 13 earthquake zones out of 22 having $M > 6$ in the said period. The time-series graphs of these two signals exhibit transient fluctuations in amplitudes in the form of spikes.

2. Experimental arrangement

The transmitted signal at frequencies 19.8 kHz and 40 kHz have regularly been recorded over the last several years from Kolkata (lat: 22.56°N, long: 88.5°E). For the reception of these signals, a straight horizontal copper wire of 8 SWG having 120 m length has been used in the form of an inverted L type antenna. The antenna, installed 30 m above the ground, is capable of receiving vertically polarized transmitted signals in the ELF–VLF bands. The LF transmitted signals are recorded by computerized data acquisition system through a PCI 1050, 16 channel 12 bit DAS card. These are then processed and stored in a computer. The r.m.s. value of the filtered data are analyzed regularly using Origin 5.0 software. The receiver system is presented by the block diagram (Fig. 1).

3. Observation and Interpretations

Fig. 2 depicts the earthquake zones along with the transmitting stations of two frequencies. Time-series graphs for these two transmitted signals during a normal day, several days earlier than the

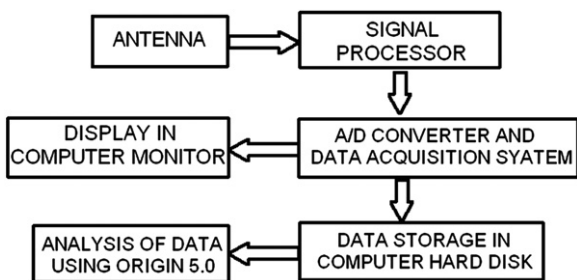


Fig. 1. Diagram of the ELF-VLF receiving system at Kolkata (lat: 22.56°N, long: 88.5°E).

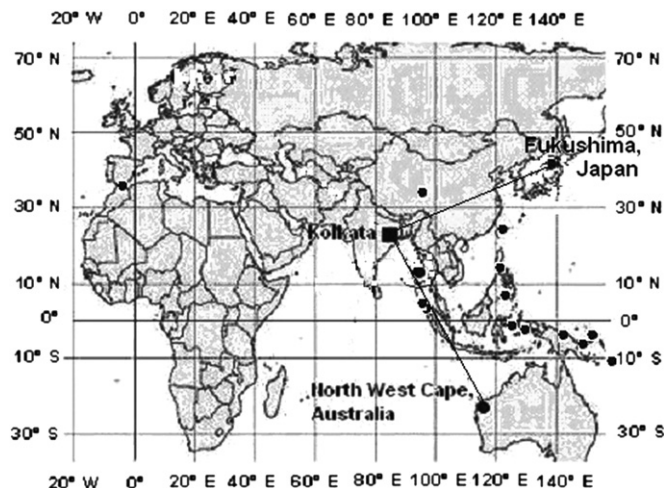


Fig. 2. Propagation paths of VLF subionospheric transmitted signals along with different earthquake zone.

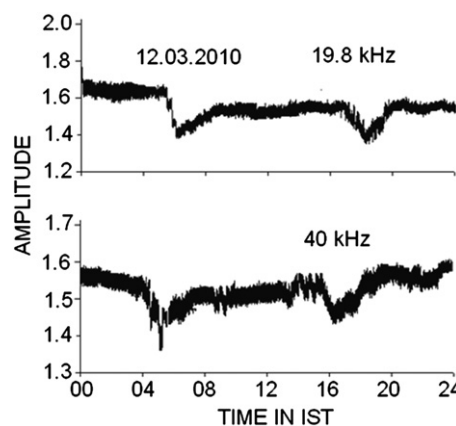


Fig. 3. Normal day record of 19.8 kHz and 40 kHz transmitted signals in a meteorologically clear day. Date: March 12, 2010.

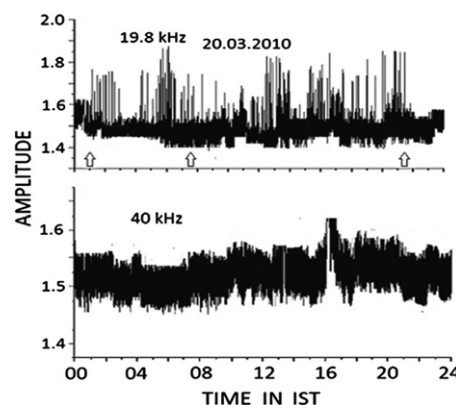


Fig. 4. Diurnal variation of 19.8 kHz and 40 kHz transmitted signals observed over Kolkata. Date: March 20, 2010.

earthquake day of March 20, 2010, are shown in Fig. 3. The normal day means meteorologically and geophysically clear day and there is no occurrence of any earthquake having $M > 5$. This figure shows the clear-cut diurnal variations with sunrise and sunset effects. Nighttime level is somewhat greater than the daytime level. Transient variations in the form of spikes are absent. Figs. 4–8 represent the time-series graphs of amplitudes of these two transmitted signals at different dates of occurrence of the earthquakes. The signals consist of a large

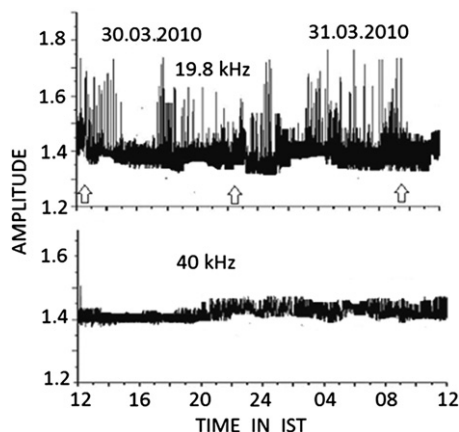


Fig. 5. Diurnal variation of 19.8 kHz and 40 kHz transmitted signals observed over Kolkata. Date: March 30, 2010 and March 31, 2010.

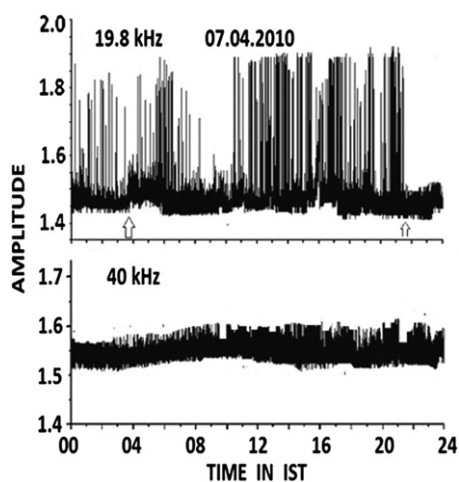


Fig. 6. Diurnal variation of 19.8 kHz and 40 kHz transmitted signals observed over Kolkata. Date: April 07, 2010.

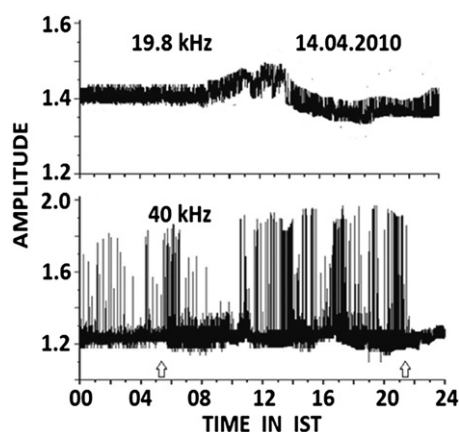


Fig. 7. Diurnal variation of 19.8 kHz and 40 kHz transmitted signals observed over Kolkata. Date: April 14, 2010.

number of transient variations in the form of remarkable spikes. The commencement of spikes, time of earthquakes and disappearance of spikes are shown by vertical arrowheads. The commencement time of occurrence of spikes is several hours earlier than the commencement of earthquakes or around the time of earthquakes. The number of

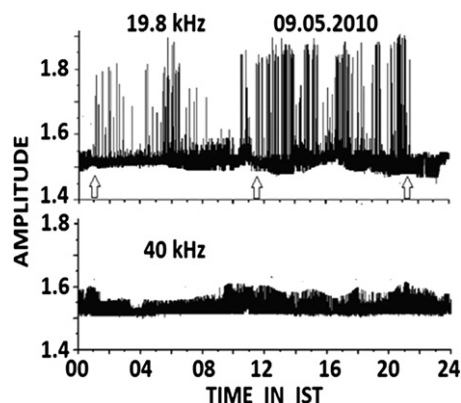


Fig. 8. Diurnal variation of 19.8 kHz and 40 kHz transmitted signals observed over Kolkata. Date: May 9, 2010.

spikes per hour is termed as intensity of spikes. The intensity varies from one earthquake to the other. The date-wise occurrence of 22 earthquakes with magnitude (M), depth and time (IST) along with their Source–Receiver distances (D) and Source–Transmitter distances and also M/D ratio are presented in Table 1. The amplitude of spikes is very much dependent on the magnitude of the earthquake, distance from the source to receiver and depth. From the tabulated data, it is observed that the intensity of the transient fluctuations show higher magnitude for higher M/D values. The commencement times of the spikes with respect to the commencement of earthquakes are shown in Table 2. Most of the cases showed the commencement of spike event precedes the earthquakes by around 10 h. The variation in spike heights indicates the relative strength of different earthquakes. The earthquake that falls on or near to the receiver–transmitter signal path produced stronger spikes as compared to the others. Higher M/D ratios have been observed when spikes are of higher amplitude. From Fig. 5, it is found that high amplitude and dense spikes occurred in the recordings of 19.8 kHz signal. These are not seen in the recording of 40 kHz signal for the earthquake of $M=6.7$ on March 30, 2010 at Andaman island (lat: 13.66°N, long: 92.83°E). Between these two transmitted signals, only 19.8 kHz signal passes this earthquake zone before reaching the receiver, and that is why the dense spikes are observed in the recording of 19.8 kHz signal. The 40 kHz signal comes to the receiver from Japan through different wave-paths. The distance of epicenter of this earthquake from Kolkata is 1090 km with M/D ratio 61.47×10^{-4} . Very dense and high magnitude spikes are observed in the recordings of 19.8 kHz transmitted signals from Australia due to earthquake of $M=7.8$ occurred on April 07, 2010 at Indonesia (lat: 2.36°N, long: 97.13°E) at a distance of 2432 km from Kolkata (Fig. 6). M/D value for this earthquake is 32.07×10^{-4} . The China (lat: 33.22°N, long: 96.67°E) earthquake of $M=6.9$ occurred on April 14, 2010 at a distance of 1430 km from Kolkata having $M/D=48.25 \times 10^{-4}$ affecting the 40 kHz signal (Fig. 7). Similar results are recorded on 19.8 kHz signal due to the occurrence of Indonesia (lat: 3.9°N, long: 96.1°E) earthquake having $M=7.4$ on May 9, 2010 (Fig. 8). The source to receiver distance for this earthquake is 2230 km and $M/D=33.18 \times 10^{-4}$. Rest of the spiky time scale graphs are self explanatory. In the time scale, the spikes occurred in the duration of the order of a few minutes. The experimental site is situated at a distance of 12 km from the nearest town, free from big and small industries, and dense locality. So, the occurrence of man-made and other industrial noise is not possible. The power supply system for the receiver is thoroughly checked and no fault or any leakage was detected. So, the nature of the spikes does not depend on any of those causes. Also, the nature of the spikes and their characteristic separations are completely different from the local thunderstorm transient variations or from any other effects, e.g., solar flare, meteor shower, geomagnetic storms (De et al., 2010).

Table 1

Date-wise occurrence of 22 earthquakes along with the descriptions of different connecting parameters.

Date	Time (IST)	Depth (Km)	Magnitude, M	Region	Affected frequency (kHz)	Distance from Kolkata (22.56°N 88.5°E), D (Km)	Calculated M/D value	Distance from Japan (37.37°N 140.85°E), (Km)	Distance from Australia (21.82°S 114.16°E), (Km)
20.03.2010	19:30:50	416	6.6	Papua New Guinea (3.38°S, 152.22°E)	19.8	7486	8.82×10^{-4}	4681	4589
25.03.2010	10:59:24	16	6	Mindoro, Philippines (13.82°N, 120.07°E)	19.8	3466	17.3×10^{-4}	3330	4015
26.03.2010	20:22:07	42	6.3	Atacama, Chile (27.95°S, 70.68°W)		17,840	3.53×10^{-4}	16,900	14,460
29.03.2010	03:08:28	30	6	Offshore Maule, Chile (35.38°S, 73.38°W)		17,750	3.38×10^{-4}	16,960	13,610
30.03.2010	22:24:46	34	6.7	Andaman Island, India (13.66°N, 92.83°E)	19.8	1090	61.47×10^{-4}	5416	4580
03.04.2010	04:28:09	32	6	Bio-Bio, Chile (36.17°S, 72.67°W)		17,650	3.40×10^{-4}	17,040	13,530
05.04.2010	04:10:41	10	7.2	Baja California, Mexico (32.12°N, 115.30°W)	19.8	13,430	5.36×10^{-4}	8974	15,030
05.04.2010	15:35:42	10	6.2	Molucca Sea (0.16°S, 125.01°E)	19.8	4689	13.22×10^{-4}	4479	2680
07.04.2010	03:45:02	31	7.8	Northern Sumatra, Indonesia (2.36°N, 97.13°E)	19.8	2432	32.07×10^{-4}	5917	3264
07.04.2010	20:03:03	34	6	Papua New Guinea (3.76°S, 141.93°E)	19.8	6495	9.24×10^{-4}	4575	3606
10.04.2010	22:24:24	275	6	Fiji Region (20.11°S, 176.23°W)		11,340	5.29×10^{-4}	7812	7165
11.04.2010	15:10:31	60.2	6.8	Solomon Island (10.91°S, 161.13°E)	19.8	8737	7.78×10^{-4}	5770	5135
12.04.2010	03:38:11	620	6.3	Spain (37.05°N, 3.51°W)		8690	7.25×10^{-4}	10,970	10,770
14.04.2010	05:19:39	17	6.9	Southern Quinghai, China (33.22°N, 96.67°E)	40	1430	48.25×10^{-4}	4000	6395
18.04.2010	04:45:20	45	6.3	Papua New Guinea (6.5°S, 147.3°E)	19.8	7162	8.80×10^{-4}	4924	3944
23.04.2010	15:33:08	43	6.3	Chile (37.4°S, 73.11°W)		17,600	3.58×10^{-4}	17,030	13,390
24.04.2010	13:11:05	78	6.1	Indonesia (1.9°S, 128.1°E)	19.8	5081	12.01×10^{-4}	4560	2680
26.04.2010	08:29:50	10	6.4	Southeast of Taiwan (22.3°N, 123.8°E)	40	3620	17.68×10^{-4}	2340	5016
01.05.2010	04:41:45	25	6.3	Bering Sea (60.5°N, 177.8°W)		8036	7.84×10^{-4}	3860	10,980
09.05.2010	11:29:41	50	7.4	Northern Sumatra, Indonesia (3.9°N, 96.1°E)	19.8	2230	33.18×10^{-4}	5873	3470
24.05.2010	21:48:29	588	6.2	Western Brazil (8.0°S, 71.7°W)		17,350	3.57×10^{-4}	15,390	16,640
31.05.2010	15:46:02	32	6	Philippines (7.0°N, 124.0°E)	19.8	4174	14.37×10^{-4}	3782	3379

The average spike height of different earthquakes from the recorded data is shown in Table 3. Spike heights as observed during March 20, 2010–May 31, 2010 for 13 earthquakes with all individual $M > 6$ are represented by bar diagram for the two frequencies in Figs. 9 and 10. The amplitude is maximum for the earthquake with larger M/D value. The bars with different heights indicate the precursory and post seismic effects at these transmitting frequencies. The diurnal pattern observed in Fig. 3 are absent in the records of the earthquake occurrence dates (Figs. 4–8).

4. Discussion

It is evident that electromagnetic emissions are observed frequently before earthquakes as high noise level in VLF and sometimes in LF band. During the last few decades, it is felt that pre-seismic electromagnetic phenomena may be a tool for short-term prediction of the occurrence of any earthquake. Pre-seismic electromagnetic signals in various frequency ranges have been analyzed. The outcome of those efforts showed temporal correlations between seismic electromagnetic signals and the occurrence of earthquakes. The electromagnetic signals are observed to be coming out from the epicentral zones (Asada et al., 2001; Hattori, 2004). The relationship between the anomalous electromagnetic

signals and earthquakes, however, has not yet been established and the nature of such signals is still not clear due to insufficient observational data and theoretical background.

Though, there are reports of electromagnetic emissions detected in air and/or underground before large earthquakes or volcanic eruptions, unfortunately, such measurements are often being plagued by contamination from other sources of noise. An electrode system is, therefore, developed that is effective at filtering out atmospheric background noise. Fujinawa and Takahasi (1990) detected anomalous electromagnetic signals several hours before the occurrence of large earthquakes near Ito city, Japan, about 150 km from the location of the electrodes. They have also detected anomalous signals about one day before an undersea volcanic eruption that constituted part of the same seismic swarm near Ito. The mechanism responsible for such signals is still unclear, but these results indicate that their monitoring could be valuable for the prediction of seismic activity.

Teisseyre and Ernst (2002) presented the theoretical considerations on electromagnetic radiation caused by dislocation dynamics in the preseismic micro-crackings located in an earthquake preparation zone. The preseismic microcrack activity may be followed by main break, the earthquake. The dynamics of micro-sources are related to the accelerated motion of

Table 2
Time of commencement of spikes with respect to the occurrence of earthquakes.

Date	Time (IST)	Affected frequency (kHz)	Precursory time	Duration of spikes after commencement of earthquakes	Calculated M/D value	Distance from Japan (37.37°N 140.85°E), (Km)	Distance from Australia (21.82°S 114.16°E), (Km)
20.03.2010	19:30:50	19.8	6 h 45 min	14 h	8.82×10^{-4}	4681	4589
25.03.2010	10:59:24	19.8	10 h	11 h	17.3×10^{-4}	3330	4015
26.03.2010	20:22:07				3.53×10^{-4}	16,900	14,460
29.03.2010	03:08:28				3.38×10^{-4}	16,960	13,610
30.03.2010	22:24:46	19.8	10 h	12 h	61.47×10^{-4}	5416	4580
03.04.2010	04:28:09				3.40×10^{-4}	17,040	13,530
05.04.2010	04:10:41	19.8	1 h	18 h 15 min	5.36×10^{-4}	8974	15,030
05.04.2010	15:35:42	19.8	12 h 15 min	7 h	13.22×10^{-4}	4479	2680
07.04.2010	03:45:02	19.8	8 h	18 h	32.07×10^{-4}	5917	3264
07.04.2010	20:03:03	19.8	24 h 20 min	1 h 40 min	9.24×10^{-4}	4575	3606
10.04.2010	22:24:24				5.29×10^{-4}	7812	7165
11.04.2010	15:10:31	19.8	12 h	6 h 30 min	7.78×10^{-4}	5770	5135
12.04.2010	03:38:11				7.25×10^{-4}	10,970	10,770
14.04.2010	05:19:39	40	8 h	16 h 30 min	48.25×10^{-4}	4000	6395
18.04.2010	04:45:20	19.8	absent		8.80×10^{-4}	4924	3944
23.04.2010	15:33:08				3.58×10^{-4}	17,030	13,390
24.04.2010	13:11:05	19.8	8 h	10 h	12.01×10^{-4}	4560	2680
26.04.2010	08:29:50	40	10 h	15 h	17.68×10^{-4}	2340	5016
01.05.2010	04:41:45				7.84×10^{-4}	3860	10,980
09.05.2010	11:29:41	19.8	11 h 30 min	10 h	33.18×10^{-4}	5873	3470
24.05.2010	21:48:29				3.57×10^{-4}	15,390	16,640
31.05.2010	15:46:02	19.8	12 h	12 h	14.37×10^{-4}	3782	3379

Table 3
Visual study of average spike heights of different earthquakes from the recorded data.

Date	Frequency (kHz)	Average height of all spikes above spike ambient level (mV)
20.03.2010	19.8	1.2
	40	0.5
25.03.2010	19.8	1.0
	40	0.6
26.03.2010	19.8	0.7
	40	0.3
29.03.2010	19.8	0.6
	40	0.4
30.03.2010	19.8	1.1
	40	0.6
03.04.2010	19.8	0.7
	40	0.5
05.04.2010	19.8	0.8
	40	0.65
07.04.2010	19.8	1.4
	40	0.9
10.04.2010	19.8	1.0
	40	0.7
11.04.2010	19.8	1.3
	40	0.9
12.04.2010	19.8	0.6
	40	1.1
14.04.2010	19.8	0.5
	40	1.32
18.04.2010	19.8	1.0
	40	1.05
23.04.2010	19.8	0.7
	40	0.8
24.04.2010	19.8	1.2
	40	1.0
26.04.2010	19.8	0.7
	40	1.3
01.05.2010	19.8	0.6
	40	0.6
09.05.2010	19.8	1.36
	40	0.8
24.05.2010	19.8	0.8
	40	0.4
31.05.2010	19.8	1.22
	40	0.6

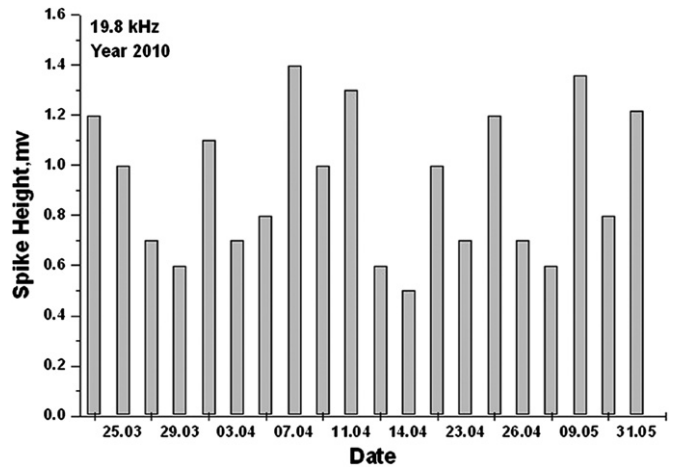


Fig. 9. Variation of spike heights above the ambient level on 19.8 kHz due to different earthquakes.

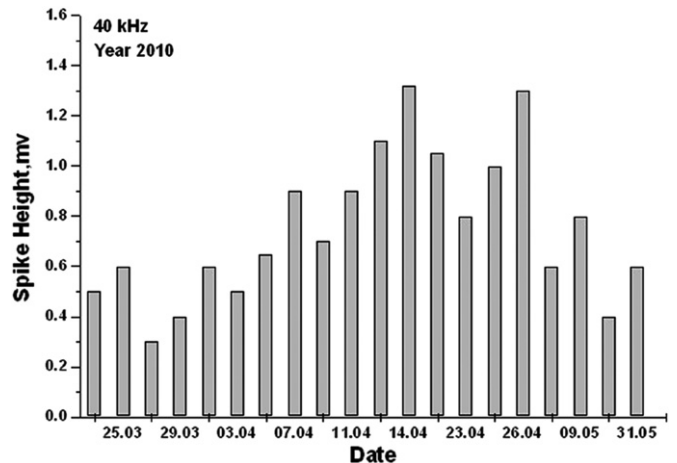


Fig. 10. Variation of spike heights above the ambient level on 40 kHz due to different earthquakes.

dislocations and to coalescences of the opposite dislocation arrays (micro-cracks). The examples of the numerically simulated induction and radiation fields are given there. They cited records of L'Aquila Geophysical Observatory recording system operating at frequencies of 10, 20 and 40 kHz.

Transient electric currents that flow in the Earth's crust are proposed to account for many non-seismic pre-earthquake signals (Freund et al., 2006). They showed that when stresses to one end of a block of igneous rocks are applied, two currents flow out of the stressed rock. When large volume of rocks are given ever increasing stress, transient fluctuating currents of considerable magnitude would be built up in the Earth's crust prior to major earthquakes. Such sources of EM radiations are proposed to be far more powerful than any other based on piezoelectricity, fractro electrification and streaming potential.

Also, all the electromagnetic signals which are generated below a certain depth, cannot reach the earth's surface (Skin depth effect). However, it may be overcome with lower frequency electromagnetic waves. Here the possibilities will be more for reaching the Earth's surface due to smaller skin depth. Underground water diffusion in a region associated with deformation of the crust prior to earthquake raises its electrical conductivity (Ishido and Mizutani, 1981). Thus, to explain the electromagnetic radiation associated with earthquakes and volcanic activities, it is necessary to calculate the attenuation of ELF/VLF waves in dry crust and wet soil.

The electric field of electromagnetic waves may be expressed as

$$\vec{E} = \vec{E}_0 \exp[j(\omega t + \vec{k} \cdot \vec{r})] \quad (1)$$

where \vec{k} is the wave vector given by $k^2 = \varepsilon\mu\omega^2 - j\sigma\mu\omega$, ω is the angular wave frequency; \vec{r} is the radial vector from the radiation source; μ is the permeability; ε is the dielectric constant and σ is the electrical conductivity. The complex wave number is given by $k = \alpha + j\beta$, ($\alpha > 0, \beta \geq 0$), α represents the propagation constant while β is the attenuation constant. The attenuation constant may be derived as

$$\beta = \omega \left\{ \frac{\varepsilon\mu}{2} (\sqrt{1 + (\sigma/\varepsilon\omega)^2} - 1) \right\}^{1/2} \quad (2)$$

The dielectric constant is expressed by $\varepsilon = \varepsilon_0 \varepsilon_r$, where $\varepsilon_0 = 1/(36\pi \times 10^9) \text{ F/m}$ is the dielectric constant or permittivity of free space and ε_r is the relative dielectric constant. The magnetic permeability μ is usually approximated by the permeability of vacuum $\mu_0 = 4\pi \times 10^{-7} \text{ H/m}$, the electric conductivities σ are of the order of 10^{-5} mho/m for dry crust.

So, $\sigma/\varepsilon\omega \gg 1$, and we get $\beta = \sqrt{\mu\omega\sigma/2}$.

The expression of β can be properly used for electromagnetic wave attenuation and it is the attenuation of electromagnetic waves in dry crust which is less than 3.9 dB/km at frequency of 19.8 kHz while it is 5.5 dB/km at 40 kHz. Therefore, if electromagnetic radiation is generated in dry crust by rock fractures over a vast region before and after the main shock of a shallow earthquake, anomalous electromagnetic waves will be observed even in the VLF band and lower LF band. The present observation is confined to 19.8 kHz and 40 kHz. The poor presence of spikes below 40 kHz may be due to propagational attenuation in the earth-ionosphere waveguide.

According to laboratory experiments, it is expected that the largest electromagnetic radiation should be observed at the time of an earthquake during largest stress change. The stored elastic energy (W) associated with deformation of rocks corresponding to an earthquake of magnitude M follows the following logarithmic relation (Bath, 1973):

$\log W = 5.24 + 1.44M$ and is supposed to be valid for $M > 5$.

For $M = 6$, $W = 7.59 \times 10^{13} \text{ J}$

The energy stored is released mainly in the short interval of time during which the largest shocks are produced. But a part of it is released in the microfracturing process.

The higher values of height and density of the spikes in the case of earthquakes nearer to the receiving station are obvious because of lower path loss. The effect is smaller in the case of signal amplitude of 40 kHz signal than that of 19.8 kHz may be at least due to two reasons—higher skin depth inside the earth and higher attenuation in the earth's atmosphere.

When considering the problem of correlation between electromagnetic emissions and earthquakes, there is a great interest in the subject for the simple reason that when the precursor event occurs, it normally does so less than a few hours before the shock.

5. Conclusion

- The transmission signal is characterized by spiky variations commencing several hours prior to the occurrence of earthquake.
- The nearer the epicenters from the receiver, the higher is the amplitudes of spikes.
- The amplitude of spikes is very much dependent on the magnitude of the earthquake.
- Greater M/D value implies the higher degree of perturbations in the ionosphere. High amplitude dense spikes are observed. This can also be justified in terms of terminator time approach (De et al., 2011).

During any large earthquake, there will be coupling between lithosphere-atmosphere and ionosphere through some probable channels, e.g., chemical channel, acoustic channel and electromagnetic (EM) channel. From chemical channel, there will be water elevation, gas emanation/radon emanation, changes in geophysical parameters which introduce chemical/conductivity changes in air resulting in a modification of the atmospheric electric field perturbing the plasma density in the ionosphere. Acoustic channel introduces excitation of atmospheric oscillations that propagate up to the ionosphere thereby modifying the ionospheric density. EM channel introduces VLF emission, ionizations, electric charge redistribution above the surface of the earth by which anomalous electric field would be generated producing large-scale irregularities. Anomalous field propagates into the inner magnetosphere and interacts with energetic particles. These particles precipitate into the lower ionosphere initiating direct heating, liberation of exo-electrons, and/or ionization of the ionosphere by seismo-ELF-VLF waves. These are detected as precursors of any vast earthquake of large M -values, which are being reported during the past two–three decades. [The energy E for an earthquake of magnitude M : For $M=7$ gives $E=2 \times 10^{15} \text{ J}$ and for $M=5$, $E=3 \times 10^{12} \text{ J}$].

From those works, although any quantitative relation between observed signals and the earthquake source parameters are lacking (Pham and Geller, 2002), the claim of background noise also fails to comply completely with the time-series records of any observed signals during the occurrence of large earthquake. The explanations about the origin of earthquake are yet to be explored. Only the outcome of the effects of their occurrences is reported till-date. For brevity, the present controversy looks like a problem of paradigm shift.

Acknowledgments

The authors are thankful to Prof. S. Kar, the then the Head, Institute of Radio Physics and Electronics, University of Calcutta, for his keen interest in the problem. They are also thankful to the

respected Reviewers for making many constructive comments, which are highly helpful to improve the manuscript. The data regarding the location and magnitudes of the significant global earthquakes which are dealt in the present paper had been collected from the following website: <http://www.imd.gov.in/section/seismo/dynamic>. Distance between two points is calculated through the website: <http://www.movable-type.co.uk/scripts/latlong.html>. These are duly acknowledged with thanks and gratitude.

References

- Asada, T., Baba, H., Kawazoe, M., Sugiura, M., 2001. An attempt to delineate very low frequency electromagnetic signals associated with earthquakes. *Earth, Planets and Space* 53, 55–62.
- Bath, M., 1973. *Introduction to Seismology*. Wiley, New York, p. 395.
- De, S.S., De, B.K., Bandyopadhyay, B., Paul, S., Haldar, D.K., Bhowmick, A., Barui, S., Ali, R., 2010. Effects on atmospheric at 6 kHz and 9 kHz recorded at Tripura during the India–Pakistan border earthquake. *Natural Hazards and Earth System Sciences* 10, 843–855.
- De, S.S., Bandyopadhyay, B., Das, T.K., Paul, S., Haldar, D.K., De, B.K., Barui, S., Sanfui, M., Pal, P., Chattopadhyay, G., 2011. Studies on the anomalies in the behaviour of transmitted subionospheric VLF electromagnetic signals and the changes in the fourth Schumann resonance mode as signatures of two pending earthquakes. *Indian Journal of Physics* 85 (3), 447–470.
- Eftaxias, K., Kopanans, J., Bogris, N., Kapisiris, P., Antonopoulos, G., Varotsos, P., 2000. Detection of electromagnetic earthquake precursory signals in Greece. *Proceedings of the Japan Academy* 76 (B), 45–50.
- Eftaxias, K., Kapisiris, P., Polygiannakis, J., Bogris, N., Kopanas, J., Antonopoulos, G., Peratzakis, A., Hadjicontis, V., 2001. Signature of pending earthquake from electromagnetic anomalies. *Geophysical Research Letters* 28, 3321–3324. <http://dx.doi.org/10.1029/2001GL013124>.
- Eftaxias, K., Kapisiris, P., Dologlou, E., Kopanas, J., Bogris, N., Antonopoulos, G., Polygiannakis, A., Peratzakis, A., Hadjicontis, V., 2002. EM anomalies before the Kozani earthquake: a study of their behaviour through laboratory experiments. *Geophysical Research Letters* 29, 1228–1231.
- Eftaxias, K., Kapisiris, P., Polygiannakis, J., Peratzakis, A., Kopanas, J., Antonopoulos, G., Rigas, D., 2003. Experience of short term earthquake precursors with VLF–VHF electromagnetic emissions. *Natural Hazards and Earth System Sciences* 3, 217–228.
- Freund, F.T., Takeuchi, A., Lau, B.W.S., 2006. Electric currents streaming out of stressed igneous rocks—a step towards understanding pre-earthquake low frequency EM emissions. *Physics and Chemistry of the Earth* 31, 389–396.
- Fujinawa, Y., Takahasi, K., 1990. Emission of electromagnetic radiation preceding the Ito seismic swarm of 1989. *Nature* 347, 376–378. <http://dx.doi.org/10.1038/347376a0>.
- Hattori, K., 2004. ULF geomagnetic changes associated with large earthquakes. *Terrestrial Atmospheric and Oceanic Sciences* 15, 329–360.
- Hayakawa, M., Molchanov, O.A., Ondoh, T., Kawai, E., 1996. The precursory signature effect of the Kobe earthquake on VLF subionospheric signals. *Journal of Communication Research Laboratory Tokyo* 43, 169–180.
- Hayakawa, M., Molchanov, O.A. (Eds.), 2002. TERRAPUB, Tokyo.
- Hayakawa, M., 2004. Electromagnetic phenomena associated with earth-quakes: A frontier in terrestrial electromagnetic noise environment. *Recent Research Development in Geophysics* 6, 81–112.
- Hayakawa, M., 2007. VLF/LF radio sounding of ionospheric perturbations associated with earthquakes. *Sensors* 7, 1141–1158.
- Hayakawa, M., Kasahara, Y., Nakamura, T., Muto, F., Horie, T., Maekawa, S., Hobara, Y., Rozhnoi, A.A., Solovieva, M., Molchanov, O.A., 2010. A statistical study on the correlation between lower ionospheric perturbations as seen by subionospheric VLF/LF propagation and earthquakes. *Journal of Geophysical Research* 115, A09305. <http://dx.doi.org/10.1029/2009JA015143>.
- Ishido, T., Mizutani, H., 1981. Experimental and theoretical basis of electrokinetic phenomena in rock–water systems and its applications to geophysics. *Journal of Geophysical Research* 86, 1763–1775.
- Izutsu, J., Oike, K., 2003. The waveforms of VLF electromagnetic waves recorded at the time of the 1995 Hyogo-ken Nanbu earthquake. *Proceedings of the Japan Academy* 79, 125–130.
- Izutsu, J., 2007. Influence of lightning on the observation of seismic electromagnetic wave anomalies. *Terrestrial Atmospheric and Oceanic Sciences* 18, 923–950.
- Kapisiris, P., Polygiannakis, J., Peratzakis, A., Nomicos, K., Eftaxias, K., 2002. VHF-electromagnetic evidence of the underlying pre-seismic critical stage. *Earth, Planets and Space* 54, 1237–1246.
- Karakelian, D., Klemperer, S.L., Fraser-Smith, A.C., Beroza, G.C., 2000. A transportable system for monitoring ultra low frequency electromagnetic signals associated with earthquakes. *Seismological Research Letters* 71, 423–436.
- Molchanov, O.A., Hayakawa, M., 2008. *Seismo Electromagnetics and Related Phenomena: History and latest Results*. TERRAPUB, Tokyo, p. 189.
- Ohta, K., Umeda, K., Watanabe, N., Hayakawa, M., 2001. ULF/ELF emissions observed in Japan, possibly associated with the Chi-Chi earthquake in Taiwan. *Natural Hazards and Earth System Sciences* 1, 37–42.
- Pham, V.N., Geller, R.J., 2002. Comment on Signature of pending earthquake from electromagnetic anomalies by K. Eftaxias et al. *Geophysical Research Letters*, 29. <http://dx.doi.org/10.1029/2002GL015328>.
- Teisseyre, R., Ernst, T., 2002. Electromagnetic radiation related to dislocation dynamics in a seismic preparation zone. *Annales Geophysicae* 45, 393–399.